

# COMPARISON OF HYBRID PI AND TEE HBT CIRCUIT TOPOLOGIES AND THEIR RELATIONSHIP TO LARGE SIGNAL MODELING

Douglas A. Teeter\*, Walter R. Curtice\*\*

\*Raytheon Electronics, Advanced Device Center, Research Laboratories,  
362 Lowell Street, Andover, MA 01810, (508) 470-9402

\*\*W. R. Curtice Consulting, 5 Berkshire Dr, Princeton Junction, NJ 08550, (609) 799-1175

## ABSTRACT

Direct comparison between the HBT small signal Tee model and the hybrid pi topology is made to 100 GHz. It is shown that a one to one correspondence exists between the two topologies, but that some of the pi model parameters exhibit a frequency dependence with respect to the Tee model parameters. Using this analysis, an enhanced Gummel Poon large signal model has been developed which extends the model accuracy (usually up to mm-wave) by properly including collector current delay, self heating, and avalanche breakdown. A collection of measured versus modeled results are given.

## INTRODUCTION

Most papers dealing with small signal HBT device performance make use of the Tee model topology[1-4]. These papers are written primarily by device developers and researchers extracting models from small signal S parameter data. The Tee model is appealing because all the model parameters can be directly tied to the physics of the device and the model fits S parameter data very well up to mm-wave frequencies. A few papers have dealt with the hybrid pi topology [5-6].

For historical reasons dating back to silicon bipolar transistor development, the Gummel Poon model is used by most bipolar circuit designers. This model is the standard large signal bipolar model available in most circuit simulators (SPICE, LIBRA, MDS, etc.). Thus, for designs which require large signal modeling, such as oscillators, power amplifiers, and mixers, the designer must use the

Gummel Poon model. Unfortunately, the Gummel Poon model reduces to the hybrid pi topology under small signal conditions, a different circuit topology from the tee model. Thus, *there is a fundamental difference between the HBT model used by device developers and that used by most circuit designers.*

This paper makes a direct comparison between the pi and tee circuit topologies. It is shown that a one to one correspondence exists between the two circuit topologies. However, the pi model parameters have a frequency dependence which becomes noticeable at high frequencies. For the devices we looked at, this occurs above 30-40 GHz. Both model topologies, when optimized, are shown to give good agreement with measured S parameter data to 50 GHz. The analysis shows that *the standard Gummel Poon large signal model can be satisfactorily used over the usable operating range of the transistor (50 GHz in our case) as long as the collector current delay is properly included in the current generator (many Gummel Poon models available in commercial simulators do not properly include this delay).* A modified Gummel Poon model which properly includes transit time delay has been developed and is described in the paper. The model is completely compatible with the standard Gummel Poon model with the important addition of transit time delay, self heating, and avalanche breakdown.

## DISCUSSION

Analysis begins by comparing the pi and tee circuit topologies. One quickly notices that the only real difference exists between the intrinsic device model, shown in

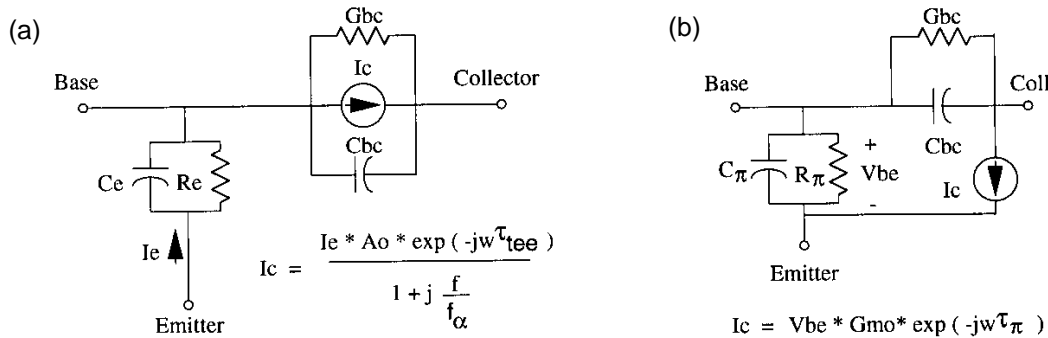


Figure 1. (a)Intrinsic HBT Tee Model, (b) Intrinsic HBT Hybrid Pi Model

figure 1. The extrinsic device model, shown in figure 2, is the same between the two topologies and therefore will have the same parameter values. Comparing the Y parameters of the intrinsic device models, expressions for the pi model parameters were derived based on the tee model values.

$$g_{mo} = \alpha_o \frac{\sqrt{G_e^2 + (\omega C_e)^2}}{\sqrt{1 + \frac{\omega^2}{\omega_\alpha^2}}} \quad (1)$$

$$\tau_\pi = \frac{\omega \tau_{tee} - \tan^{-1}(\frac{\omega C_e}{G_e}) + \tan^{-1}(\frac{\omega}{\omega_\alpha})}{\omega} \quad (2)$$

$$G_\pi = G_e - g_{mo} \cos(\omega \tau_\pi) \quad (3)$$

$$C_\pi = C_e + g_{mo} \frac{\sin(\omega \tau_\pi)}{\omega} \quad (4)$$

$$\omega_\alpha = 2\pi f_\alpha$$

To evaluate both model topologies, on wafer S parameter measurements were taken on several  $80 \mu\text{m}^2$  common emitter (CE) HBTs. The devices used a self aligned base contact for minimum base resistance and paired  $2 \times 20 \mu\text{m}^2$

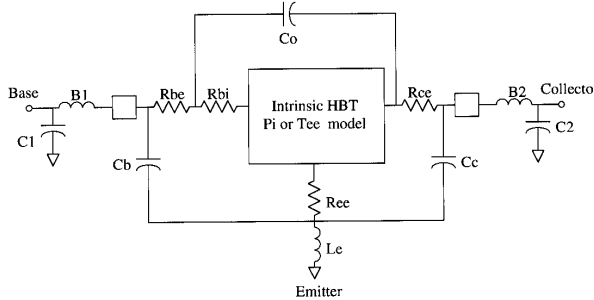


Figure 2. Extrinsic HBT Small Signal Model.

emitter fingers to minimize the extrinsic base-collector capacitance. Upon completion of the front side processing, the GaAs substrate was thinned to 2 mil to allow use of individual emitter ground vias for low emitter inductance. Intrinsic and extrinsic model parameters are given in tables I and II. Note that  $\tau_\pi$  is not necessarily equal to  $\tau_{tee}$  as explained by equation 2 and table II.

Table I: Extrinsic Device Model Parameters (3V, 39 mA)

Rbe	0.638	Rce	0.749
Ree	4.009	Rbi	6.129
Gbc	0	Cbc	0.0009 pF
Co	0.0713 pF	Le	8.28 pH
Cb	0 pF	Cc	0.0193 pF

Table II: Optimized Intrinsic Device Model Parameters (3V, 39 mA)

Tee Model	Pi Model
Re	1.23
Ce	1.6 pF
G <sub>bc</sub>	0 mS
C <sub>bc</sub>	0.0009 pF
$\alpha_o$ (Ao)	0.9511
$\tau_{tee}$	3.17 pS
f	400 GHz

The frequency dependence of the pi model parameters were compared at a number of bias points. A typical result for  $I_c=39 \text{ mA}$  ( $50 \text{ kA/cm}^2$ ) and  $V_{ce}=3 \text{ V}$  is shown in figures 3a and 3b. The frequency variation becomes noticeable above about 40 GHz. As the transit time ( $\tau_{tee}$ ) increase, the frequency at which the pi parameters are no longer constant decreases. However, the  $f_{max}$  also decreases as  $\tau_{tee}$  increases, reducing the usable upper frequency limit of the device.

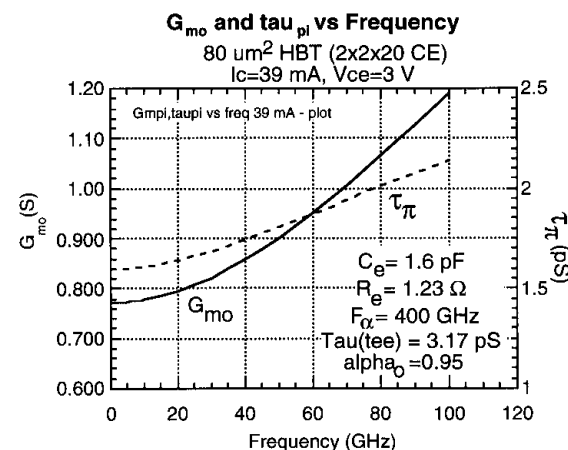
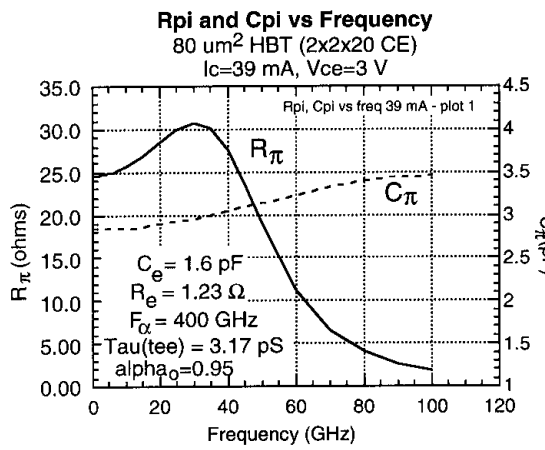


Figure 3a & 3b. Intrinsic Pi model parameters computed from T model values for an  $80 \mu\text{m}^2$  HBT.

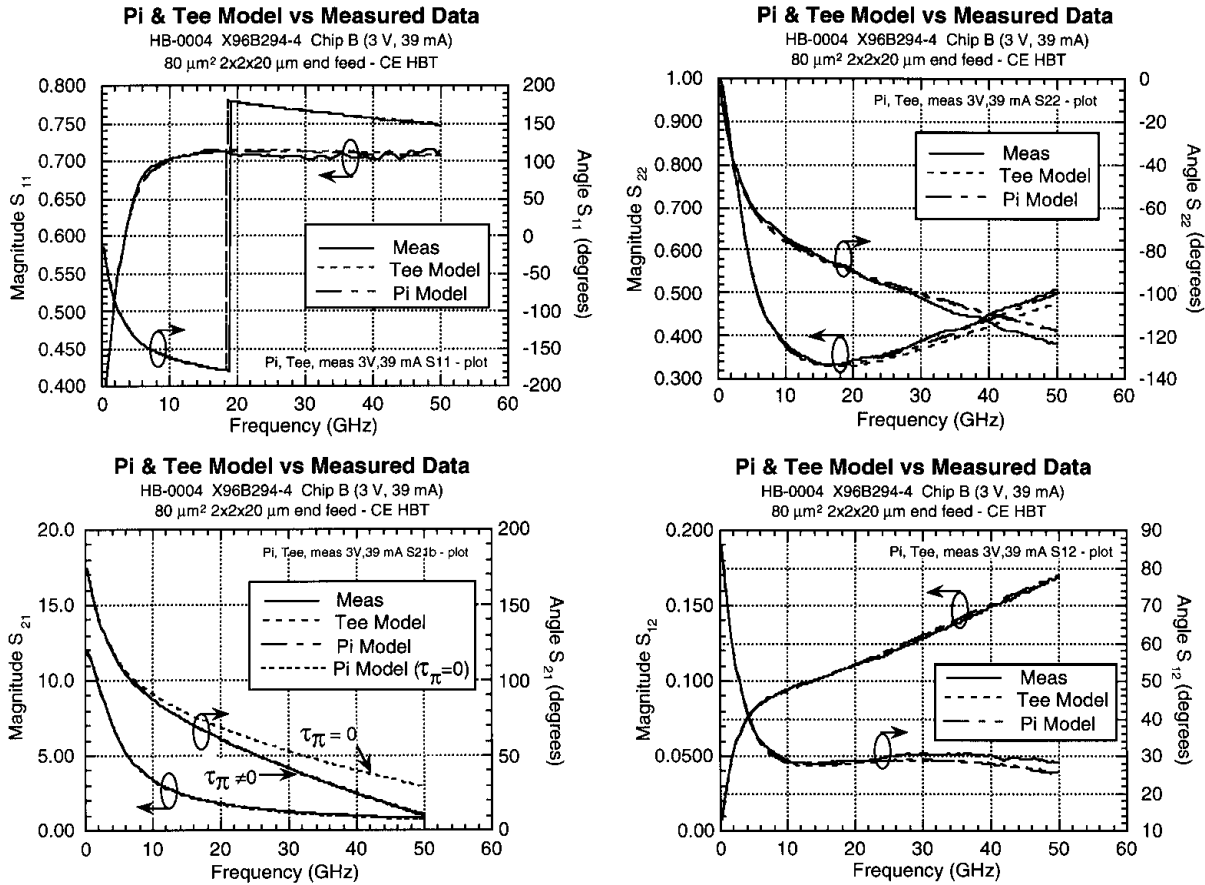


Figure 4. Comparison of measured and modeled S parameter data for an  $80 \mu\text{m}^2$  ( $2 \times 2 \times 20 \mu\text{m}$ ) HBT biased at 3V, 39 mA. a) S11 b) S22 c) S21 d) S12

Figure 4 compares measured and modeled S parameter data up to 50 GHz. Both pi and tee model topologies agree well with the measured data using frequency independent parameters as long as transit time delay is included in the equivalent circuit. Simulated S parameters of both model topologies began to differ only when

$\tau_{\text{ee}} > 2$  (above 100 GHz for the model in figures 3 and 4), well beyond the usable range of the transistor or the probable validity of either model. Figure 4c also shows the disagreement in measured and modeled S21 phase which results when one forces  $\tau = 0$  during the optimization. Many Gummel Poon models available in commercial harmonic balance simulators reduce to the  $\tau = 0$  case under small signal conditions.

To test the validity of the pi topology under large signal conditions, a modified Gummel-Poon model was developed for use in Libra 6.0 [7] [8]. Figure 5 shows the model topology. It is identical to the standard Gummel Poon model with the impor-

tant addition of avalanche breakdown, collector current delay, and self heating effects. Time delay in the collector current generator is accounted for using the "get\_delay\_v" feature available for Libra 6.0 senior elements [8]. The nonlinear model equations and their thermal dependence

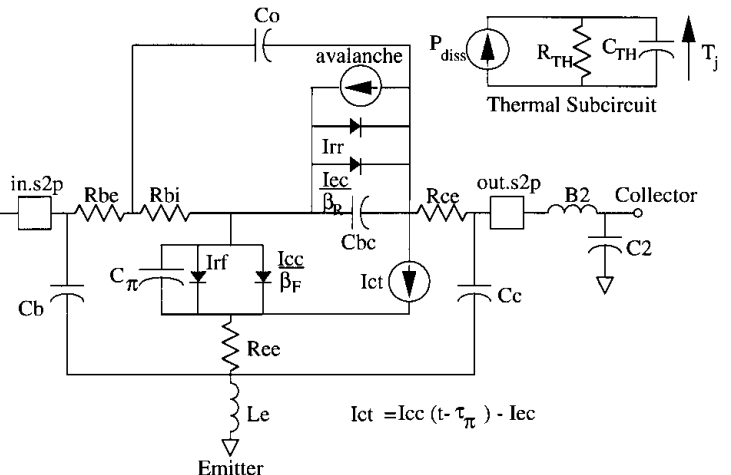


Figure 5. Modified Gummel Poon Large Signal Model with collector current delay (transit time)

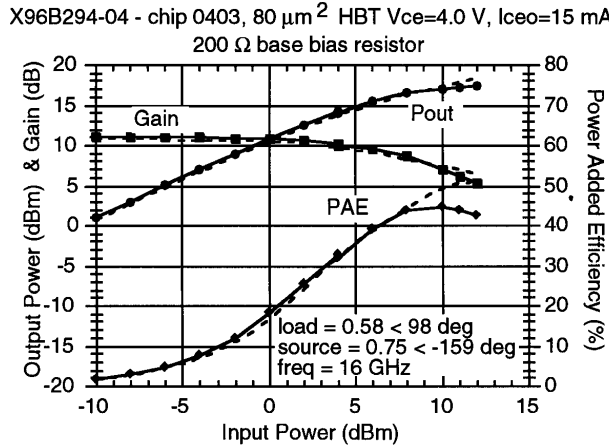


Figure 6. Measured (solid) vs modeled (dashed) power transfer characteristics at  $V_{ce}=4$  V,  $I_c=15$  mA, and 16 GHz for an  $80 \mu\text{m}^2$  HBT (class AB operation).

may be found in reference [9]. Self heating is treated in the same manner as found in [10] [11]. Table III summarizes the large signal model parameters. The parasitic element values are given in Table I.

Table III - Large Signal Model parameters for an  $80 \mu\text{m}^2$  HBT

ISS	1.40e-20 A	F <sub>c</sub>	0.96	Tau	1.8 pS	V <sub>jc</sub>	1.26 V
BF	15	IKF		TF	3.9 ps	M <sub>jc</sub>	0.55
BR	1	IKR		TR	3.0 ns	X <sub>cjc</sub>	0.03
NF	1.33	NE	1.94	C <sub>je</sub>	94.5 fF	R <sub>th</sub>	1130 °C/W
NR	1.31	NC	1.67	V <sub>je</sub>	1.30 V	C <sub>th</sub>	885 pF
ISE	7.81e-17 A	VAF		M <sub>je</sub>	0.23	E <sub>g</sub>	1.68 eV
ISC	8.35e-16 A	VAR		C <sub>jc</sub>	123 fF	X <sub>TB</sub>	-1

Swept power measurements were taken at 16 GHz to assess the validity of the model. Figure 6 shows a typical measured versus modeled result. Simulations were also performed at 38 GHz to assess the importance of the collector current delay time. As one can see from figure 7, inclusion of  $\tau$  in the model can have a significant impact on the predicted gain (and hence output power).

## CONCLUSIONS

This paper demonstrates that a one to one correspondence exists between the small signal HBT pi and tee circuit topologies. While the parameter values for the pi model are not frequency independent with respect to the tee model parameters, good fits to measured S parameter data can be obtained using frequency independent model parameters for the useful frequency range of the device. Thus, the commonly used Gummel Poon large signal model can be utilized over the usable frequency range of the HBT (usually up to mm-wave) provided that the collector current delay is properly included in the model.

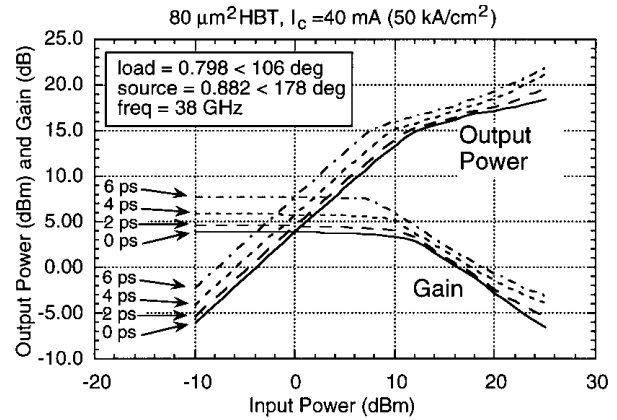


Figure 7: Simulated output power and gain at 38 GHz for an  $80 \mu\text{m}^2$  HBT for various values of  $\tau$ .

## ACKNOWLEDGMENTS

The authors wish to thank Ron Bourque, Joe Gering, and Marc Snow for measurement support and technical guidance.

## REFERENCES

- [1] D. Pehlke and D. Pavlidis, "Evaluation of the Factors Determining HBT High Frequency Performance by Direct Analysis of S-Parameter Data," *IEEE Trans. MTT*, Dec. 1992, pp. 2367-2373.
- [2] S. Spiegel, et. al., "Extraction of the InP/GaInAs Heterojunction Bipolar Transistor Small-Signal Equivalent Circuit," *IEEE Trans. Electron Devices*, June 1995, pp 1059-1064.
- [3] C. Wei, et. al., "Direct Extraction of Equivalent Circuit Parameters for Heterojunction Bipolar Transistors," *IEEE Trans. MTT*, Sept. 1995, pp 2035-2039.
- [4] U. Schaper and B. Holzapfl, "Analytical Parameter Extraction of the HBT Equivalent Circuit with T-Like Topology from Measured S-Parameters," *IEEE Trans. MTT*, March 1995, pp. 493-498.
- [5] D. Wu, et. al., "Unique Determination of AlGaAs/GaAs HBT's Small-Signal Equivalent Circuit Parameters," *1993 GaAs IC Symposium*, pp 259-262.
- [6] D. Costa, et. al., "Direct Extraction of the AlGaAs/GaAs Heterojunction Bipolar Transistor Small-Signal Equivalent Circuit," *IEEE Trans. on Electron Devices*, Sept. 1991, pp. 2018-2024.
- [7] W.R. Curtice Consulting, 5 Berkshire Dr, Princeton Junction, NJ 08550, (609) 799-1175.
- [8] HP EESOF Libra Series IV user's manual.
- [9] Giuseppe Massobrio and Paolo Antognetti, *Semiconductor Device Modeling with Spice*, McGraw-Hill, Inc., 1993, chapter 2.
- [10] P. Grossman, et. al. "Large Signal Modeling of HBTs Including Self-Heating and Transit Time Effects," *IEEE Trans. MTT*, March 1992, pp. 449-464.
- [11] L. Camnitz, et. al. "An Accurate, Large Signal, High Frequency Model for GaAs HBTs," *1996 GaAs IC Symposium*, pp 303-306.